

# CO<sub>2</sub> Conversion into Methanol Using Granular Silicon Carbide ( $\alpha$ 6H-SiC): A Comparative Evaluation of 355 nm Laser and Xenon Mercury Broad Band Radiation Sources

Mohammed Ashraf Gondal · Mohammed Ashraf Ali ·  
Mohamed Abdulkader Dastageer · Xiaofeng Chang

Received: 27 July 2012 / Accepted: 23 September 2012 / Published online: 11 October 2012  
© Springer Science+Business Media New York 2012

**Abstract** Granular silicon carbide ( $\alpha$ 6H-SiC) was investigated as a photo-reduction catalyst for CO<sub>2</sub> conversion into methanol using a 355 nm laser from the third harmonic of pulsed Nd:YAG laser and 500 W collimated xenon mercury (XeHg) broad band lamp. The reaction cell was filled with distilled water,  $\alpha$ 6H-SiC granules and pressurized with CO<sub>2</sub> gas at 50 psi. Maximum molar concentration of methanol achieved was 1.25 and 0.375 mmol/l and the photonic efficiencies of CO<sub>2</sub> conversion into methanol achieved were 1.95 and 1.16 % using the laser and the XeHg lamp respectively. The selectivity of methanol produced using the laser irradiation was 100 % as compared to about 50 % with the XeHg lamp irradiation. The band gap energy of silicon carbide was estimated to be 3.17 eV and XRD demonstrated that it is a highly crystalline material. This study demonstrated that commercially available granular silicon carbide is a promising photo-reduction catalyst for CO<sub>2</sub> into methanol.

**Keywords** Photo-catalytic reduction ·  $\alpha$ 6H-SiC · CO<sub>2</sub> conversion into methanol · Laser based photo catalysis · Green chemistry

## 1 Introduction

Carbon dioxide is one of the major contributors to global warming. Over the last 100 years, the concentration of the atmospheric CO<sub>2</sub> has recorded an alarming rise of about 30 % mainly due to the increased consumption of fossil fuels for automotives, power generation and heating equipment. The potential dangers of the reckless usage of the green house gases and their terrifying consequences in global warming are well understood and governments and international organizations have taken serious steps to minimize the release of CO<sub>2</sub> and other green house gases into the atmosphere. The examples of such earnest commitments of the international organizations to minimize global warming are the Kyoto agreement in environmental issues, and implementation of the carbon quotas and carbon trading regulations by many countries [1].

Any process that converts the surplus of CO<sub>2</sub> into some high-value compounds such as methanol will be the most ideal proposition not only to minimize the CO<sub>2</sub> release into atmosphere but also to convert it into a useful product. Research in this area will definitely help in reducing the release of CO<sub>2</sub> in the atmosphere and the consequent dangerous environmental issues like adverse climatic change, global warming and the Green house effect. Also converting the undesired excess of CO<sub>2</sub> into the most sought after energy products like methanol will definitely be a welcome move. This is a kind of two birds with one stone proposition as this kind of research targets both energy and the environmental crisis at the same time.

---

M. A. Gondal (✉) · M. A. Dastageer · X. Chang  
Laser Research Group, Physics Department and Center  
of Excellence in Nanotechnology, King Fahd University  
of Petroleum and Minerals, Dhahran 31261, Saudi Arabia  
e-mail: magondal@kfupm.edu.sa

M. A. Ali  
Center for Refining and Petrochemicals, Research Institute,  
King Fahd University of Petroleum and Minerals,  
Dhahran 31261, Saudi Arabia

X. Chang  
College of Materials Science and Technology, Nanjing  
University of Aeronautics and Astronautics,  
Nanjing 211100, China

With the ever increasing global requirement for energy on one side and ever shrinking global energy sources on the other side, research efforts are underway to develop environmentally friendly sustainable and renewable energy sources. In this line, transformation of CO<sub>2</sub> into useful products such as methanol, hydrogen, and methane is highly advantageous and it will fulfill both goals: reduction of greenhouse gases for global warming issue as well as providing alternate renewable energy sources [2].

As CO<sub>2</sub> is a very stable and inert molecule, Most of the processes for converting it into value added compounds require a lot of energy. Recent research has shown that photo-catalysis is a promising method of converting CO<sub>2</sub> into methanol; however finding a highly reactive and efficient catalyst to reduce the CO<sub>2</sub> molecule remains a challenge. Moreover, this process should be economically viable and environmentally friendly to adopt this process for an industrial scale, which demands the usage of inexpensive and abundant material and renewable energy sources.

Semiconductor catalysts have been effectively used for many photo-chemical processes such as bacterial disinfection, water purification, recycling of organic dyes, conversion of methane into methanol and so on [3]. When the photon energy ( $h\nu$ ) of the incident radiation is more than that of the band gap ( $E_g$ ) of the semiconductor, the electrons from the valence band will be excited to the conduction band leaving positively charged holes in the valence band (VB). The electron hole pairs, generated by photo-excitation can move to the surface of semiconductor particle to form a highly oxidizing radicals like  $\bullet$ OH (hydroxyl radical) and  $\text{}^{-}\text{O}_2$  (super-oxide radical). This process can pursue a number of chemical pathways that could lead to variety of reaction products.

Several pathways and numerous catalytic materials have been investigated by several researchers to develop efficient catalytic materials for conversion of CO<sub>2</sub> into useful products such as ethers, methanol, dimethylether [4], propylene, ethylene, methane, CO<sub>2</sub> based copolymers [5, 6] and organic and inorganic carbonates [7].

Wang and coworkers [8] applied copper doped titania-silica nanostructured photo-catalysts and achieved relatively good CO<sub>2</sub> conversion efficiency. Titania-based photo-catalysts have been used for CO<sub>2</sub> photo-catalytic reduction in the presence of H<sub>2</sub>O to produce chemicals such as methanol or methane [9, 10]. TiO<sub>2</sub> film coated on optical fiber using a dip-coating method was utilized for CO<sub>2</sub> conversion as well [11]. A number of catalysts prepared by loading indium on the oxides of vanadium, niobium and tantalum have demonstrated quite good improvement in their photo-catalytic activities due to a decrease in their band gap [12–14]. It has been demonstrated that nickel oxide loading promotes the photo-

catalytic activity of different catalysts for water splitting [15, 16]. Chen et al. [17] have successfully synthesized In TaO<sub>4</sub> photo-catalyst using an aqueous sol-gel method and it was modified by loading with NiO and used for the photo-catalytic reduction of CO<sub>2</sub> into methanol [18]. WO<sub>3</sub> has been used also as a photo-catalyst in the UV region [19, 20]. Silicon carbide has rarely been used in the photo-catalytic conversion of CO<sub>2</sub> into hydrocarbons.

In this work, granular  $\alpha$ 6H-SiC was applied as a photo-catalyst in the conversion of CO<sub>2</sub> into methanol in the presence of 355 nm monochromatic laser radiation and a broad band radiation source and the relative merit of these two radiations in the production yield of methanol converted from CO<sub>2</sub> and the photonic efficiencies were investigated. A special reaction cell aiming at the optimum interaction of radiation and the catalyst was designed. CO<sub>2</sub> dissolved in distilled water at 50 psi pressure and the  $\alpha$ 6H-SiC catalyst was placed inside the water and exposed to incident radiation. The 355 nm laser radiation was generated from the third harmonic of pulsed Nd:YAG laser and the broadband band source was a xenon mercury (XeHg) lamp. The production yield (conversion of CO<sub>2</sub> into methanol) was estimated by Gas Chromatographic analysis (GC) of the water sample taken at a regular time intervals of irradiation. The GC peak was calibrated to the known molar concentrations of methanol in the millimole/liter (mM) scale. The maximum concentration of methanol produced was 1.25 mM with the laser irradiation and 0.375 mM with the XeHg lamp irradiation. The maximum photonic efficiency of CO<sub>2</sub> into methanol with the 355 nm laser radiation was 1.95 and 1.16 % with the XeHg lamp. This enhancement of photonic efficiency with the laser is attributed to the inherent qualities of the laser beam. In addition to the enhanced yield, the selectivity in the case of the laser irradiation is very impressive as methanol is practically the only product in the laser based photo-reaction compared to other accompanying products in the case of the broadband source. In order to estimate the band gap and other characteristics of  $\alpha$ 6H-SiC, the optical characterization and XRD of the photo-catalyst was carried out. The results of the study demonstrated that the granular silicon carbide is a promising catalytic material for photo-catalytic conversion of CO<sub>2</sub> into methanol in the presence of UV laser radiation.

## 2 Experimental

### 2.1 Chemicals and Materials

Silicon carbide (Saint-Gobain, USA) with the grain size of 1.5  $\mu$ m size granules was used without any further processing. CO<sub>2</sub> gas with the purity of 99.997 % was obtained

from a local supplier and the distilled water of very high purity was obtained from our plant. The methanol used for the calibration of GC was of spectroscopic grade and was obtained from Lab-Scan analytical Sciences.

## 2.2 Characterization

The Spectrophotometer for diffuse reflectance spectra, the spectrofluorometer for photoluminescence (PL) spectra and XRD system X-ray diffraction of the  $\alpha$ 6H-SiC, were used for this work. These studies provided an estimation of the band gap energy ( $E_g$ ) and the crystallographic nature of the photo-catalytic material. Diffuse Reflectance UV-Vis measurement was carried out using the JASCO 670 spectrophotometer equipped with integration sphere (JASCO) to find the band gap energy of  $\alpha$ 6H-SiC. The granular  $\alpha$  6H-SiC was stuck on the carbon tape in the form of a very thick film and this was used as a specimen for the diffused reflectance. Unlike the specular reflectance spectrum in diffuse reflectance spectrum, the reflection from the powder sample surface was diffused in all directions and was collected using the integration sphere, which directed the reflected light to the detector. For PL spectra, a Shimadzu 530 PC spectrofluorometer with a 150 W Xenon lamp source was used and the grating groove density was 1,200 lines/mm. The sample for the PL spectrum was in a suspension form, where the sample is powdered in a mill and the suspension in distilled water was made after sonicating it for 30 min. The excitation wavelength for the obtained PL spectrum was 355 nm. The XRD data in the present work was recorded on a Shimadzu XRD-6000, X-ray diffractometer with Cu K $\alpha$  X-ray radiation ( $\lambda = 1.5406 \text{ \AA}$ ) from a broad focus tube at the 40 kV electrical voltage and 30 mA current. The scanning speed for data collection was 2  $^\circ$ /min. and the angle scanned was 20 $^\circ$ –80 $^\circ$  ( $2\theta$ ). The sample was mounted on a glass substrate with the help of carbon paste.

## 2.3 Photo-Catalytic Reaction

The photo-catalytic reaction cell and its setup have been described in our earlier publications [21]. The photo-catalytic reactor is a cylindrical stainless steel cell with quartz windows on the top to enable the transmission of 355 nm UV radiation. At the bottom of the cell there is a gas inlet with a needle valve that let the CO<sub>2</sub> gas passing through the distilled water in the cell and almost at the same level at the opposite side there is an outlet fixed with the rubber septum in order to dispense the sample through the syringe. The whole cell is kept on a magnetic stirrer that constantly replenishes the photo-catalyst in the path of radiation. Care has been taken not to let the water level to go very much

higher than the level of the catalyst platform in order to have better interaction of radiation with the photo-catalyst. Since the quantity of sample taken for GC at each time was around 4.0  $\mu$ L, the water level did not decrease due to sample withdrawing from the reaction cell. The reaction cell was cleaned, dried and a predetermined amount of  $\alpha$ 6H-SiC granular material (3 g) was loaded along with 100 mL distilled water and then was tightly closed and checked for leaks up to 50 psi pressure. High purity CO<sub>2</sub> gas (99.99 %) was introduced through reactor inlets and the reactor pressure was maintained at 50 psi. Prior to turning on the pulsed laser, CO<sub>2</sub> gas was purged into 100 mL water containing 3.0 g of  $\alpha$ 6H-SiC granules for 30 min in order to saturate the contents of the reactor with CO<sub>2</sub>. After a predetermined irradiation time, water samples were withdrawn from the reactor using syringe without opening the reactor and were subjected to GC analysis.

The laser (355 nm) used for this study was the third harmonic of the pulsed Nd:YAG laser (Model Spectra Physics GCR 250–10) the laser operated at 10 Hz. and the pulse width of  $\sim$ 8 ns. Throughout this study the laser pulse energy of 40 mJ/pulse was used. The laser beam was routed with the high power UV reflecting mirrors/dichroic mirrors so that the beam enters from the top of the cell and also appropriate lens is used to slightly expand the beam to the same diameter of the catalyst platform when it reaches there. Although the laser pulse energy was quite stable it was monitored throughout the experiment with the 50–50 beam splitter and the laser energy meter (Coherent). The broad band source is the Oriel with the 500 W XeHg lamp equipped with a beam collimator and 90 $^\circ$  beam turning mirror.

## 2.4 Product Analysis

The water samples were analyzed for methanol and other hydrocarbons by means of gas chromatography equipped with a flame ionization detector (FID). The separation of the components was carried out on an Rtx-Wax column (dimensions: 30 m  $\times$  0.32 mm  $\times$  0.32 mm) obtained from Restek, using temperature programmed conditions. For the analysis, 4.0  $\mu$ L of product sample was injected into the gas chromatograph and the operating conditions were as follows: Oven temperature was set at 40  $^\circ$ C which was then increased to 90  $^\circ$ C at 5  $^\circ$ C/min heating rate and then increased to 180  $^\circ$ C at the rate of 50  $^\circ$ C/min to elute all the components from the column before injecting another sample. The injector and detectors both were set at 200  $^\circ$ C and helium was used as carrier gas. The total analysis run time was 11.8 min. A calibration plot was developed for methanol standard solution in distilled water for calculating the amount of methanol produced as a function of irradiation time.

### 3 Results and Discussion

#### 3.1 Characterization of Photo-catalyst

Semiconductor material  $\alpha$ 6H-SiC is an indirect band gap material having a band gap energy ranging between 2.3 and 3.3 eV, depending on the various polytypes that exist. The band gap energy of 3C-SiC ( $\beta$ SiC) is 2.35 eV and that of 4H-SiC ( $\alpha$ -SiC) and 6H-SiC ( $\alpha$ -SiC) are respectively 3.28 and 3.08 eV [22]. The alpha silicon carbide ( $\alpha$ -SiC) is the most commonly encountered polymorph; it is formed at temperatures greater than 1,700 °C and has a hexagonal crystal structure (similar to Wurtzite). The diffuse reflectance, PL and the XRD characterization were carried out for the  $\alpha$ 6H-SiC used in this study.

##### 3.1.1 Diffuse Reflectance Spectra and Band Gap Determination

The major characteristic that influences the performance of the semiconducting material is its band gap energy, the energy between the top level of the valance band and the bottom level of the conduction band. The band gap energy is the key factor of the semiconducting material for any application including photo-catalysis, where the energy of the incident photon in the photo-catalytic reaction should be more than that of the band gap energy. Commonly, for powdered samples the absorption spectrum of the sample in the aqueous suspension form is used to determine the band gap energy. In the case of the absorption spectrum of semiconductor in suspension, the scattered light will interfere with the absorption phenomenon resulting in inaccurate absorption data. In order to avoid this problem associated with the UV-Vis absorption spectrum, a diffuse reflectance spectrum of the powder sample was carried out and the Kubelka–Munk function [23–25] was used to find the band gap energy. In diffuse reflectance, unlike in the case of specular reflectance, the light reflected off the sample is a kind of diffused light and is collected by the integrating sphere and directed to the detector.

For thick powdered samples like SiC, the Kubelka–Munk function for reflectance is expressed as  $F(R) = (1 - R)^2 / 2R = K/S$ , where  $R$  is the reflectance,  $K$  apparent absorption coefficient and  $S$  apparent scattering coefficient. The  $K$  and  $S$  are related to the true absorption coefficient  $\alpha$  and scattering coefficient  $\sigma$  respectively as  $\alpha(\nu) = \eta K$  and  $\sigma(\nu) = \chi S$ , where  $\eta$  and  $\chi$  are the constant. Also we know for the indirect band gap material like  $\alpha$  6H- SiC, the scattering coefficient  $\alpha(\nu) = (E - E_g)^2 / E$ , where  $E$  is the photon energy and  $E_g$  is the band gap energy. Since  $\alpha(\nu)$  is related to  $F(R)$ , we express that the Kubelka–Munk function  $F(R)$  is proportional to  $(E - E_g)^2 / E$ , where  $E$  is the photon energy and  $E_g$  is the band gap energy and this expression can be

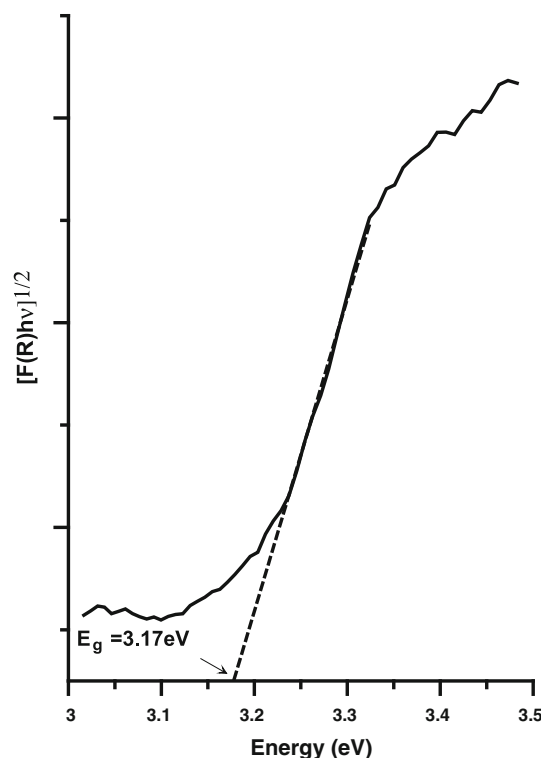


**Fig. 1** Diffuse reflectance spectra of  $\alpha$ 6H-SiC, showing the band gap energy

linearised to find the  $E_g$  from the reflectance data as proposed by Tauc [26]. Figure 1 depicts the diffuse reflectance spectrum where  $(F(R) * E)^{1/2}$  versus  $E$  is plotted and the band gap energy estimated is 3.17 eV approximately corresponds to 389 nm of wavelength. This band gap energy is closer to the band gap energy of the  $\alpha$ 6H-SiC of polytype  $\alpha$ 6H-SiC. This justifies the use of 355 nm (3.47 eV) laser as incident radiations for  $\alpha$ 6H-SiC in our study which is capable of promoting the electron from the valance to conduction band and thereby triggering photo-catalytic process. The broad band source we used in our study was a XeHg lamp and it has the considerable irradiance above the band gap energy.

##### 3.1.2 Photoluminescence Spectral Measurement

Photoluminescence measurements at room temperature for  $\alpha$ 6H-SiC were carried out with powdered suspension in distilled water and the PL spectrum is depicted in Fig. 2. The excitation wavelength used for the PL spectrum was 355 nm monochromatic light source, whose photon energy is higher than the band gap energy and also this was the wavelength we used for the photo-catalytic reaction. The PL spectrum has the emission peak centered at 444 nm (2.78 eV), which is less than the band gap energy of  $\alpha$  6H-SiC (3.17 eV). This indicates that there is some kind of non radiative recombination of energy states that deactivates the system to the lower energy level and subsequently from

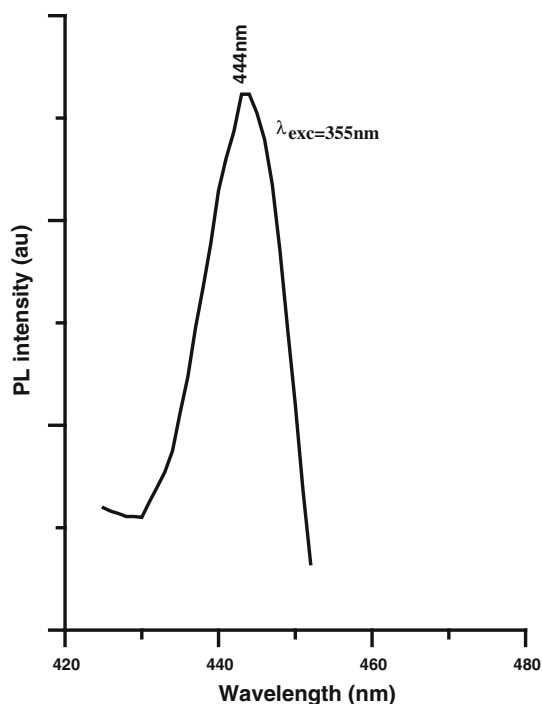


**Fig. 2** Photoluminescence plot of  $\alpha 6\text{H-SiC}$ , showing the peak maximum at 444 nm. The excitation wavelength was 355 nm

there the final radiative transition takes place [27]. This blue emission of  $\alpha 6\text{H-SiC}$  at 444 nm is visibly checked under 355 nm laser radiation and also in the broad band light source, the blue emission was quite visible in both cased in powder as well as in the suspension form.

### 3.1.3 X-ray Diffraction Measurement

SiC exists in as many as 200 polytypes, identified by their Laue patterns among these 3C, 4H and 6H are the most common, where H represents the hexagonal structure and C represents the cubic structure. It is essential to identify the crystal structure of the actual SiC we used (hexagonal). The XRD of the powdered SiC with all the Miller indices labeled is shown in Fig. 3 and comparing our data with Joint Committee on Powder Diffraction Standards, JCPDS card # 29-1128, it confirms the hexagonal structure with  $a = 0.308$  nm;  $c = 1.512$  nm. The average Si–C bond lengths are 0.188 nm, with average bonds along the stacking direction is 0.189 nm [28].

## 3.2 Photo-catalytic Reactions

When the photon energy ( $h\nu$ ) of the incident radiation is more than that of the band gap ( $E_g$ ) of the semiconductor, the electron hole pairs, generated by photo-excitation can move to the surface of semiconductor particle to form

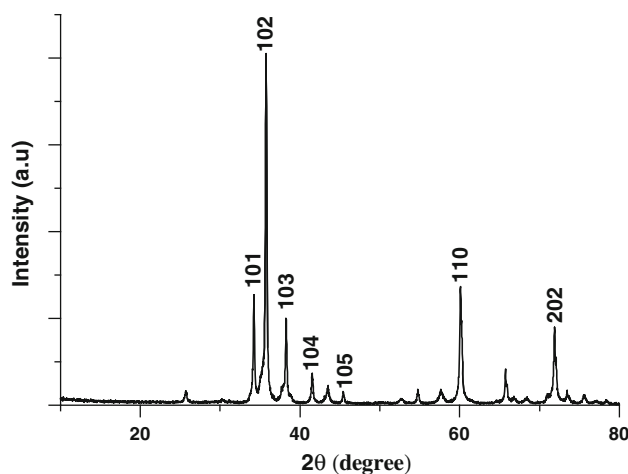
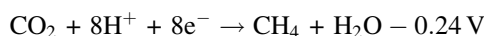
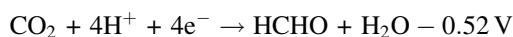
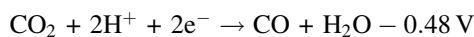
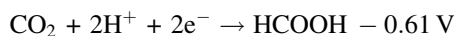
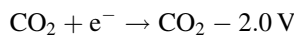
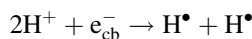
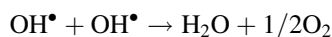
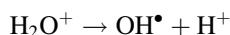
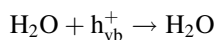


**Fig. 3** X-ray diffraction pattern of  $\alpha 6\text{H-SiC}$ . The Miller indices are labeled

highly oxidizing radicals like  $\bullet\text{OH}$  (hydroxyl radical) and  $\text{O}_2^-$  (super-oxide radical). This process can pursue a number of chemical pathways that could lead to variety of reaction products. The possible pathways during conversion of  $\text{CO}_2$  in aqueous solution are the followings



### 3.2.1 Conversion of $\text{CO}_2$ into Methanol

Methanol is produced from dissolved  $\text{CO}_2$  in distilled water through photo-catalytic process in the presence of semi-conducting photo-catalyst, granular  $\alpha 6\text{H-SiC}$  using monochromatic laser and broad band radiation sources. The monochromatic wavelength was a 355 nm high energy pulsed laser beam and the broad band source was 500 W collimated XeHg radiation source. The methanol produced through the photo-catalytic process was verified and quantified with the help of gas chromatogram (GC) which shows the retention time of 2.45 min for methanol standard for the gas chromatographic parameters selected and the

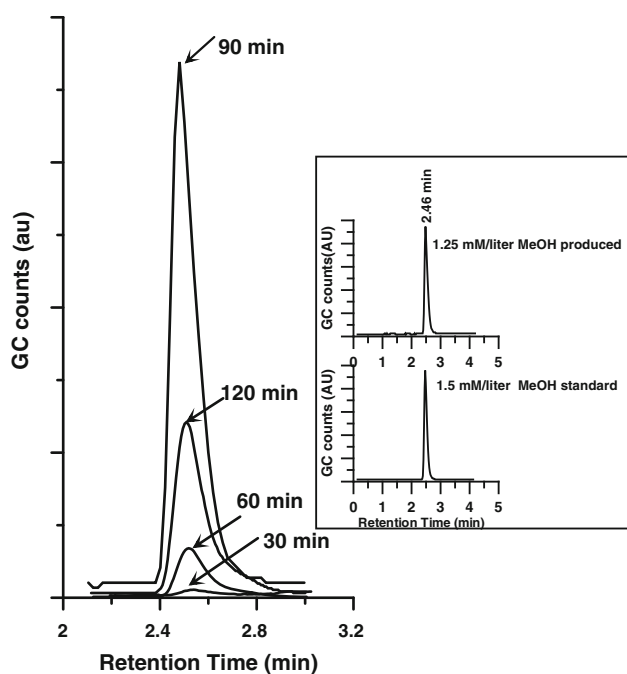


**Fig. 4** Gas chromatograms of reaction products collected at 30–120 min irradiation in the presence of 355 nm laser having 40 mJ/pulse energy. The inset shows the comparison of retention time of GC peaks with the methanol standard and it is at 2.46 min

column used. Figure 4 shows gas chromatographic peak of the methanol produced in the photo-catalytic process with 355 nm laser having pulse energy of 40 mJ/pulse as a radiation source obtained at four different irradiation times. The gas chromatographic peaks of methanol produced as a result of broad band radiation from a collimated 500 W XeHg lamp are depicted in Fig. 5. The data presented in both Figs. 4 and 5 was achieved using 3.0 g of granular  $\alpha$ 6H-SiC in the photo-catalytic reactor contained high purity CO<sub>2</sub> at 50 psi pressure. In the case of the XeHg lamp source, the catalyst was kept almost 20 cm from the lamp exit so that optimum intensity of collimated light falls on the entire catalyst surface, whereas in the case of the laser the beam was slightly expanded to cover the whole surface of the catalyst. The irradiance of the collimated lamp source at 20 cm was measured with the light meter and it was 340 klx at 20 cm distance (at the very spot of the photo-catalyst).

### 3.2.2 Product Analysis and Quantification of Methanol

The ordinates of Figs. 4 and 5 are in the instrument dependent arbitrary units of gas chromatographic peak area counts and are presented only to indicate the general trend of the level of formation of methanol with the irradiation time. On comparing the gas chromatographic peak areas in Fig. 4 (for 355 nm laser), which clearly show the growing

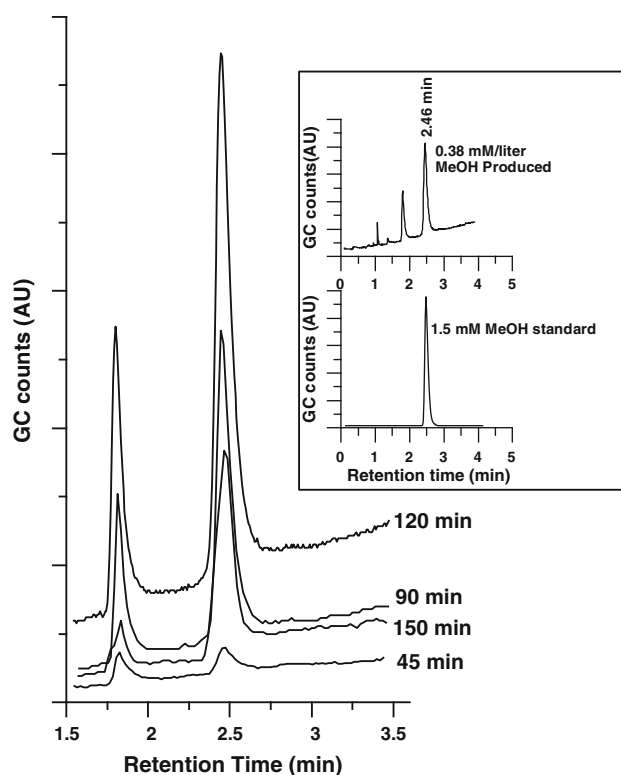


**Fig. 5** Gas chromatograms of reaction products collected at 45–120 min irradiation in the presence of the XeHg lamp having 500 W. The inset shows the comparison of retention time of GC peaks with the methanol standard and it is at 2.46 min

methanol concentration with the irradiation time (30, 60, and 90 min) and gets the maximum methanol concentration in 90 min of irradiation and starts to fall. Similar trends are also observed in Fig. 5 with the difference that the maximum methanol concentration is attained in 120 min of irradiation, and decreased afterward. The levels of gas chromatographic peak area counts in Figs. 4 and 5, clearly indicate that the methanol production yield from the photo-catalysis using  $\alpha$ 6H-SiC semiconductor catalyst in conjunction with 355 nm laser radiation is significantly more than that produced using a broadband XeHg lamp source which is attributed to the monochromatic and other inherent superior qualities of intense laser radiation. It is worth mentioning that at this level of discussion, the gas chromatographic retention time was used for a qualitative analysis only. In the forthcoming discussions, we have use area under the GC peak to quantify the methanol concentrations and also for calibrating of the methanol. The insets in Figs. 4 and 5 are the GC peaks of 1.5 M of diluted methanol standard and that of the methanol produced by photo-catalysis and the retention time for both are exactly 2.46 min, which proves that the product recorded in the chromatogram is methanol produced from the photo-catalytic process. Another striking difference between the

355 nm laser irradiation and the broad band XeHg lamp source irradiation is the selectivity. Contrary to the results plotted in Fig. 5, Fig. 4 has almost no other GC peaks besides the methanol peak at 2.46 min retention time in the gas chromatograph, which suggests that the methanol is the only product which was obtained through the laser induced photo-catalytic CO<sub>2</sub> conversion process, possibly because of the monochromatic characteristic of the pulsed laser. Thus, the laser irradiation has almost 100 % methanol selectivity. In the case of the XeHg irradiation source based CO<sub>2</sub> conversion, other hydrocarbons were also obtained and thus the methanol selectivity was lower as compared to the laser based methanol selectivity because of the monochromatic property of the pulse laser used. The monochromatic radiation may produce photogenerated electrons with centered reduction energy, therefore high selectivity of methanol can be achieved from CO<sub>2</sub>. However, photogenerated electrons with different reduction energy can be produced under exposure of broad band XeHg irradiation source which possesses many wavelengths and therefore different hydrocarbon products are generated.

In order to present the concentration of the methanol produced in a meaningful way we did the calibration of the GC with known concentrations of methanol standard in mM, where the area under the GC peak was taken as an instrumental parameter in the calibration curve. The calibration curve in Fig. 6 shows a linear trend as in the case of most GC calibrations. The diluted methanol standard with different concentrations were prepared with extreme care

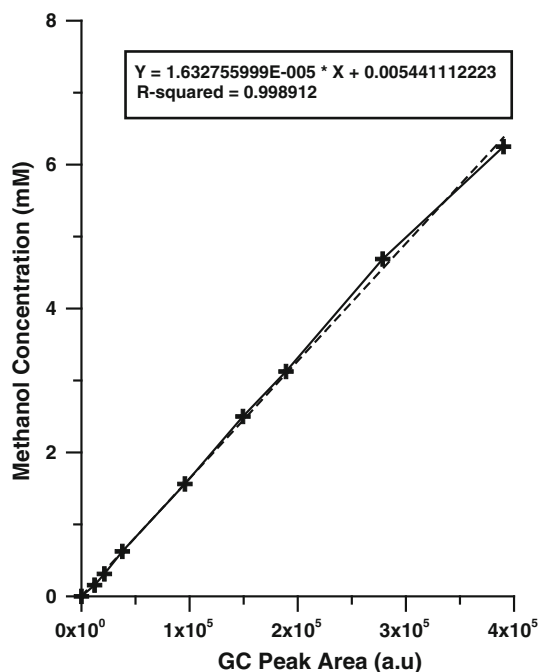


**Fig. 6** Calibration plot of pure methanol standard as a function of peak area

from a stock solution and many blank runs were done in the GC before injecting each standard sample to make sure there was no trace of the previous injection in the GC persists in the GC column. Figure 7 shows the concentration variation of the photo-catalytic process of converting CO<sub>2</sub> into methanol with laser as well as a broadband lamp radiation. In Fig. 7 (dashed line), we notice that the laser radiation produces maximum yield at 90 min and the concentration was 1.25 mM, and afterwards the concentration declines. The same is the case with the lamp but he maximum concentration of 0.375 mM is achieved after 120 min and further exposure makes the concentration decline.

It can be found from Fig. 7 that after a certain level of methanol concentration is reached, the concentration of methanol starts decreasing, which is possibly due to the existence of photocatalytic oxidation of methanol over SiC semiconductor with positive VB position [21]. When methanol was produced in a substantial amount, it is adsorbed on the surface of the photo-catalyst and then undergoes oxidation processes and this phenomenon has been observed and explained by other groups [29–31]. It is worth noticing that a pair of competitive reactions (i.e. photo-reduction and photo-oxidation) exists in this photochemical process (as depicted in Fig. 8). At the very beginning, the photoreduction rates might be faster than that of photooxidation because of the low concentration of methanol produced ( $k_r > k_o$ ). Therefore it is deduced that the photoreduction process should be a rate control step.

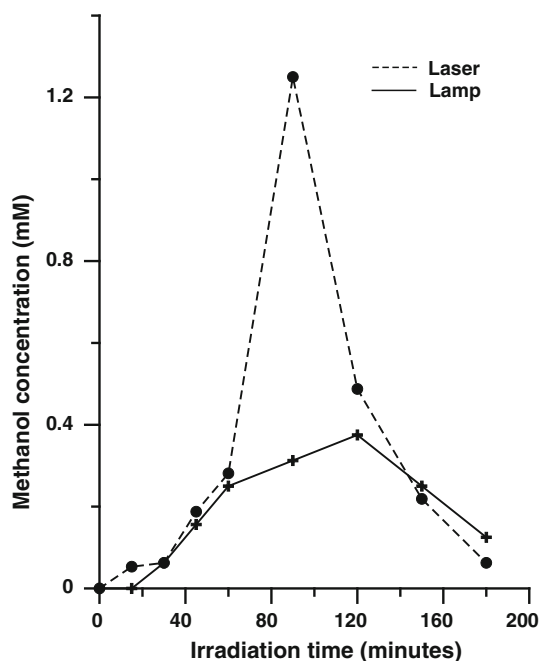


**Fig. 7** Methanol molar concentration versus irradiation time. The dashed line for the laser and the solid line for the XeHg lamp source

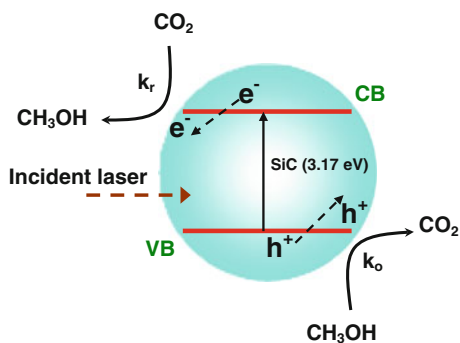


**Fig. 8** Schematic illustration of the competitive photooxidation and photoreduction reactions in the photochemical process

According to the Langmuir–Hinshelwood mechanism, the oxidation rate is strongly dependent on the concentration of methanol, that is, increased methanol concentration facilitates the oxidation process. After the concentration of methanol reaches to a certain value, the rate control step is replaced by photooxidation rather than photoreduction ( $k_r < k_o$ ) thus the methanol concentration decreases.

Like any chemical reaction, the product of the chemical reaction reaches a maximum concentration; the methanol concentration also reaches to a maximum level after a certain time of photo-reaction. In our case, it is possible that a kind of simultaneous competing reaction is responsible for the depletion of produced methanol. As the reverse reaction is simultaneously taking place and the photo-reaction that produces methanol was initially stronger than the oxidation reaction due to favorable experimental conditions resulting in the increase of methanol concentration with irradiation time. Table 1 lists the methanol concentration, photonic efficiency both in the case of 355 nm laser irradiation as well as XeHg broad band source.

To understand the declining methanol concentration with time after a certain exposure time, known arbitrary

**Table 1** Methanol concentration produced and the photonic efficiency determined using the laser and the XeHg lamp irradiation study

Irradiation time (min)	500 W XeHg Lamp		355 nm Laser (70 mJ/pulse)	
	MeOH concentration (mM)	Photonic efficiency (%)	MeOH concentration (mM)	Photonic efficiency (%)
15	0	0	0.053	0.3
30	0.062	0.19	0.062	0.45
45	0.156	0.48	0.187	0.58
60	0.250	0.77	0.281	0.65
90	0.312	0.96	1.252	1.95
120	0.375	1.16	0.487	0.56
150	0.250	0.77	0.218	0.2
180	0.125	0.39	0.062	0.038

concentration of methanol in water was irradiated in the presence of  $\alpha$ 6H-SiC separately with 355 nm laser radiation (40 mJ/pulse) and the XeHg light source. The GC analysis was carried out after a certain irradiation time and the depletion of methanol present in water under the same experimental condition is presented in Fig. 9 as initial arbitrary concentration of methanol taken as 100 % and subsequent decline of methanol concentration with irradiation time as the reduced percent (done with the area under the curve of GC Peaks). The solid line indicates the depletion curve for 355 nm laser and the solid line for the XeHg lamp. The depletion of methanol with irradiation time shows a sharper decline in the case of the laser than the XeHg lamp, which indicates that some kind of radiation based degradation has taken place, which competed with the photo-catalytic production of methanol. In our previous study, we have investigated the decay of methanol where we hypothesized that most of the methanol was converted into hydrogen [32].

### 3.2.3 Photonic Efficiency of CO<sub>2</sub> Conversion into Methanol

In order to estimate the level of CO<sub>2</sub> conversion into methanol in the presence of  $\alpha$ 6H-SiC semiconductor catalyst and light source, we estimated the photonic efficiency

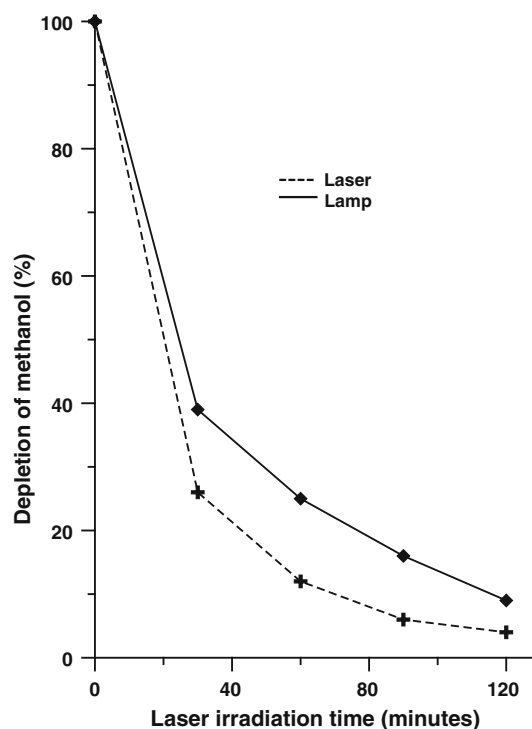


**Fig. 9** Depletion of methanol in water with by in the presence of 50 mJ of 355 nm laser (dashed line) and a 500 W XeHg lamp (solid line)



of the process. Now that we know the actual concentrations of methanol at different irradiation times of the photo-catalytic process, the number of methanol molecules can be estimated from the molar concentrations and Avogadro's number. In the case of the laser, the number of photon of wavelength 355 nm with the laser pulse energy 40 mJ/pulse and repetition rate of 10 Hz can be calculated to be  $5.364 \times 10^{19}$  photons/min. For the broad band lamp a radiation intensity of 340 klux was measured at 20 cm from the lamp and these corresponds to  $1.3 \times 10^{19}$  photons/min. From the number of methanol molecules produced for a certain irradiation time and the number of photons applied we can calculate the photonic efficiency of the photo-catalytic conversion of CO<sub>2</sub> into methanol.

The number of methanol molecules produced is expected to increase with the number of photons used up for the reaction and as the irradiation time increased the number of photons available for the reaction will also increase. However, after a certain time, like any other chemical reaction, a certain kind of thermodynamic or chemical equilibrium is expected to reach and the product concentration should remain constant unless the reverse reaction or any other reaction that depletes the product concentration occurs. As a result, the photonic efficiency was also expected to increase and get a maximum at equilibrium and begin to decline as the production of methanol is reduced and the number of photons available goes on increasing with time. This trend is quite obvious in the plot showing

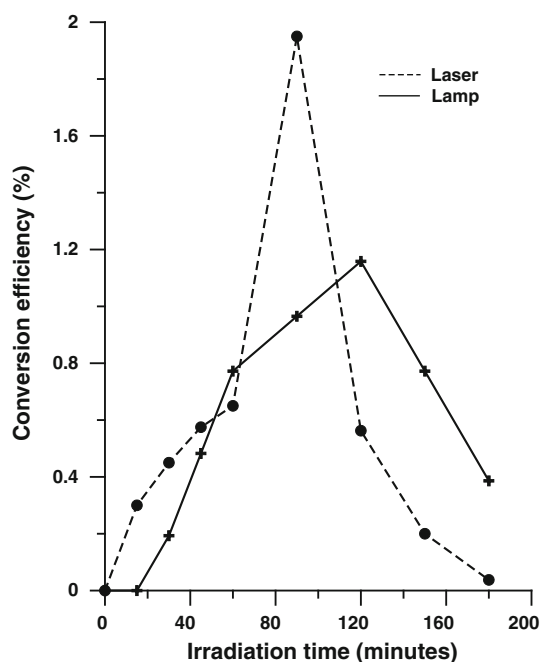


**Fig. 10** photonic efficiency versus irradiation time in the photo-catalytic production of conversion of CO<sub>2</sub> into methanol in water with by in the presence of 50 mJ of 355 nm laser (dashed line) and the 500 W XeHg lamp (solid line)

photonic efficiency versus irradiation time (dashed line) in Fig. 10. The maximum photonic efficiency estimated in the photo-catalytic process of CO<sub>2</sub> conversion into methanol was 1.95 % after 90 min of irradiation with 40 mJ/pulse of 355 nm laser radiations and 1.16 % after 120 min of exposure from the 500 W XeHg lamp. The achievement of high conversion using the laser irradiation is attributed to the inherent qualities of the laser beam (monochromaticity and high intensity).

#### 4 Conclusions

In this study, the photonic efficiency and conversion efficiency of photo-catalytic conversion of CO<sub>2</sub> into methanol using granular  $\alpha$ 6H-SiC semiconductor in the presence of pulsed 355 nm laser radiation (pulse energy 40 mJ/pulse) and a 500 W XeHg were investigated. The methanol produced from the photocatalytic reaction was identified and further quantified using methanol standard for calibration. The maximum photonic efficiency determined in the photo-catalytic process of CO<sub>2</sub> conversion into methanol was 1.95 % after 90 min of irradiation with 40 mJ/pulse of 355 nm laser radiation and 1.16 % after 120 min of exposure from a 500 W XeHg lamp. The maximum photonic efficiency achieved so far with best catalyst is less than 1.5 % as reported by others [18, 33]. In addition to the enhanced yield, the selectivity of the laser irradiation is very attractive since methanol was the only product obtained in the laser based photo-catalytic reaction as compared to the XeHg broad band radiation source. The band gap of  $\alpha$ 6H-SiC was estimated using diffuse reflectance spectrum, while other characteristics were determined by PL and XRD of the photo-catalyst. The band gap energy of  $\alpha$ 6H-SiC was estimated to be 3.17 eV while the XRD demonstrated that  $\alpha$ 6H-SiC is a highly crystalline material.

**Acknowledgments** This work was financially supported by King Fahd University of Petroleum and Minerals under the Deanship of Scientific research through approved the Laser Research Group projects # RG1011-1 and RG1011-2. The continuous support of the Physics Department is also acknowledged.

#### References

- Melanie O (2012) Law Libr J 104:179
- Raj NT, Iniyar S, Goic R (2011) Renew Sustain Energy Rev 15:3640
- Gondal MA, Bagabas AA, Dastageer MA, Khalil A (2010) J Mol Catal A 323:78
- Xu Y, Yan SZ, Ye TQ, Zhang Z, Li QX (2011) Acta Phys Chim Sin 27:1926
- M.A. Scibioh, B. Viswanathan, Research Signpost: Trivandrum, 2002

6. Darensbourg DJ (2010) *Inorg Chem* 49:10765
7. Smith YR, Subramanian V, Viswanathan B (2010) *Bentham Science Publishers* 1:217
8. Wang WN, Park J, Biswas P (2011) *Catal Sci Technol* 1:593
9. Rajalakshmi K, Jeyalakshmi V, Krishnamurthy KR, Viswanathan B (2012) *Ind J Chem* 51A:411
10. Dey GR, Belapurkar AD, Kishore K (2004) *J Photochem Photobiol A Chem* 163:503
11. Jeffrey CS, Lin H (2005) *Intl J Photoener* 7:115
12. Zou Z, Ye J, Arakawa H (2000) *Chem Phys Lett* 332:271
13. Zou Z, Ye J, Arakawa H (2001) *Mater Res Bull* 36:1185
14. Ye J, Zou Z, Arakawa H, Oshikiri M, Shimoda M, Matsushita A, Shishido T (2002) *J Photochem Photobiol A Chem* 148:79
15. Thaminimulla CTK, Takata T, Hara M, Kondo JN, Domen K (2000) *J Catal* 196:362
16. Zou Z, Ye J, Sayama K, Arakawa H (2001) *Nature* 414:625
17. Chen HC, Chou HC, Wu JCS, Lin HY (2008) *J Mater Res* 23:1364
18. Wang ZY, Chou HC, Wu JCS, Tsai DP, Mul G (2010) *Appl Catal A Gen* 380:172
19. Maruthamuthu P, Ashokkomar M, Gurunathan K, Subramanian E, Shastri MVC (1989) *Int J Hydrogen Energy* 14:525
20. Maruthamuthu P, Ashokkomar M (1989) *Int J Hydrogen Energy* 14:275
21. Gondal MA, Ali MA, Chang XF, Shen K, Xu QY, Yamani ZH (2012) *J Environ Sci Health Part A* 47:1571
22. Haeringen WV, Bobbert PA, Backes WH (1997) *Phys Stat Sol (b)* 202:63
23. Kubelka P, Munk F (1931) *Z Tech Phys (Leipzig)* 12:593
24. Kubelka P (1948) *J Opt Soc Am* 38:448
25. Mudgett PS, Richards LW (1971) *Appl Opt* 10:1485
26. Tauc J (1968) *Mater Res Bull* 3:37
27. Botsoa J, Bluet JM, Lysenko V, Sfaxi L, Zakharko Y, Marty O, Guillot G (2009) *Phys Rev B* 80:155317
28. Capitani GC, Pierro SD, Tempesta G (2007) *Am Mineral* 92:403
29. Suzuki Satoshi, Tsuneda Takao, Hirao Kimihiko (2012) *J Chem Phys* 136:024706
30. Hagen A, Barkschata JK, Dohrmann H, Tributsch (2003) *Sol Energy Mater Sol Cells*. 77:1
31. Wang Chuan-yi, Rabani Joseph, Bahnemanna Detlef W, Dohrmann Jürgen K (2002) *J Photochem Photobiol A* 148:169
32. Gondal MA, Hameed A, Yamani ZH (2004) *J Mol Catal A* 222:259
33. Kim W, Seok T, Choi W (2012) *Energy Environ Sci* 5:6066